Biomedical Optics EXPRESS

Fluorescence lifetime spectroscopy of tissue autofluorescence in normal and diseased colon measured *ex vivo* using a fiber-optic probe

Sergio Coda,[1,2,5,*] Alex J. Thompson,[1,5] Gordon T. Kennedy,[1] Kim L. Roche,[1,2] Lakshmana Ayaru,[2] Devinder S. Bansi,[2] Gordon W. Stamp,[3,4] Andrew V. Thillainayagam,[1,2,6] Paul M. W. French,[1,6] and Chris Dunsby[1,3,6]

[1]*Photonics Group, Department of Physics, Imperial College London, Prince Consort Road, London, SW7 2AZ, UK*
[2]*Endoscopy Unit, Department of Gastroenterology, Charing Cross Hospital, Imperial College Healthcare NHS Trust, Fulham Palace Road, London, W6 8RF, UK*
[3]*Department of Histopathology, Imperial College London, Du Cane Road, London, W12 0NN, UK*
[4]*Cancer Research UK London Research Institute, 44 Lincoln's Inn Fields, London, WC2A 3LY, UK*
[5]*These authors contributed equally to this work*
[6]*These authors contributed equally to this work*
[*]*s.coda@imperial.ac.uk*

Abstract: We present an *ex vivo* study of temporally and spectrally resolved autofluorescence in a total of 47 endoscopic excision biopsy/resection specimens from colon, using pulsed excitation laser sources operating at wavelengths of 375 nm and 435 nm. A paired analysis of normal and neoplastic (adenomatous polyp) tissue specimens obtained from the same patient yielded a significant difference in the mean spectrally averaged autofluorescence lifetime −570 ± 740 ps ($p = 0.021$, $n = 12$). We also investigated the fluorescence signature of non-neoplastic polyps ($n = 6$) and inflammatory bowel disease ($n = 4$) compared to normal tissue in a small number of specimens.

OCIS codes: (170.3650) Lifetime-based sensing; (300.6500) Spectroscopy, time-resolved; (300.6540) Spectroscopy, ultraviolet; (300.6550) Spectroscopy, visible; (120.3890) Medical optics instrumentation; (170.2680) Gastrointestinal.

References and links

1. R. Lambert, H. Saito, and Y. Saito, "High-resolution endoscopy and early gastrointestinal cancer...dawn in the East," Endoscopy **39**(3), 232–237 (2007).
2. P. Boyle and B. Levin, World Cancer Report 2008 (World Health Organisation - International Agency for Research on Cancer, Geneva, 2008).
3. S. H. Taplin, W. Barlow, N. Urban, M. T. Mandelson, D. J. Timlin, L. Ichikawa, and P. Nefcy, "Stage, age, comorbidity, and direct costs of colon, prostate, and breast cancer care," J. Natl. Cancer Inst. **87**(6), 417–426 (1995).
4. B. Vogelstein, E. R. Fearon, S. R. Hamilton, S. E. Kern, A. C. Preisinger, M. Leppert, Y. Nakamura, R. White, A. M. Smits, and J. L. Bos, "Genetic Alterations during Colorectal-Tumor Development," N. Engl. J. Med. **319**(9), 525–532 (1988).
5. D. K. Rex, "Risks and potential cost savings of not sending diminutive polyps for histologic examination," Gastroenterol Hepatol (N Y) **8**(2), 128–130 (2012).
6. A. Hotouras, P. Collins, W. Speake, G. Tierney, J. N. Lund, and M. A. Thaha, "Diagnostic yield and economic implications of endoscopic colonic biopsies in patients with chronic diarrhoea," Colorectal Dis. **14**(8), 985–988 (2012).
7. S. S. Cross and J. L. Stone, "Proactive management of histopathology workloads: analysis of the UK Royal College of Pathologists' recommendations on specimens of limited or no clinical value on the workload of a teaching hospital gastrointestinal pathology service," J. Clin. Pathol. **55**(11), 850–852 (2002).
8. K. Gono, T. Obi, M. Yamaguchi, N. Ohyama, H. Machida, Y. Sano, S. Yoshida, Y. Hamamoto, and T. Endo, "Appearance of enhanced tissue features in narrow-band endoscopic imaging," J. Biomed. Opt. **9**(3), 568–577 (2004).

#194923 - $15.00 USD Received 31 Jul 2013; revised 11 Oct 2013; accepted 26 Nov 2013; published 16 Jan 2014

9. N. Nakaniwa, A. Namihisa, T. Ogihara, A. Ohkawa, S. Abe, A. Nagahara, O. Kobayashi, J. Sasaki, and N. Sato, "Newly developed autofluorescence imaging videoscope system for the detection of colonic neoplasms," Dig. Endosc. **17**(3), 235–240 (2005).
10. R. Kiesslich, J. Burg, M. Vieth, J. Gnaendiger, M. Enders, P. Delaney, A. Polglase, W. McLaren, D. Janell, S. Thomas, B. Nafe, P. R. Galle, and M. F. Neurath, "Confocal laser endoscopy for diagnosing intraepithelial neoplasias and colorectal cancer in vivo," Gastroenterology **127**(3), 706–713 (2004).
11. T. D. Wang, S. Friedland, P. Sahbaie, R. Soetikno, P. L. Hsiung, J. T. Liu, J. M. Crawford, and C. H. Contag, "Functional imaging of colonic mucosa with a fibered confocal microscope for real-time in vivo pathology," Clin. Gastroenterol. Hepatol. **5**(11), 1300–1305 (2007).
12. I. Georgakoudi, B. C. Jacobson, J. Van Dam, V. Backman, M. B. Wallace, M. G. Müller, Q. Zhang, K. Badizadegan, D. Sun, G. A. Thomas, L. T. Perelman, and M. S. Feld, "Fluorescence, reflectance, and light-scattering spectroscopy for evaluating dysplasia in patients with Barrett's esophagus," Gastroenterology **120**(7), 1620–1629 (2001).
13. M. B. Wallace, L. T. Perelman, V. Backman, J. M. Crawford, M. Fitzmaurice, M. Seiler, K. Badizadegan, S. J. Shields, I. Itzkan, R. R. Dasari, J. Van Dam, and M. S. Feld, "Endoscopic detection of dysplasia in patients with Barrett's esophagus using light-scattering spectroscopy," Gastroenterology **119**(3), 677–682 (2000).
14. G. Zonios, L. T. Perelman, V. Backman, R. Manoharan, M. Fitzmaurice, J. Van Dam, and M. S. Feld, "Diffuse reflectance spectroscopy of human adenomatous colon polyps in vivo," Appl. Opt. **38**(31), 6628–6637 (1999).
15. L. B. Lovat, K. Johnson, G. D. Mackenzie, B. R. Clark, M. R. Novelli, S. Davies, M. O'Donovan, C. Selvasekar, S. M. Thorpe, D. Pickard, R. Fitzgerald, T. Fearn, I. Bigio, and S. G. Bown, "Elastic scattering spectroscopy accurately detects high grade dysplasia and cancer in Barrett's oesophagus," Gut **55**(8), 1078–1083 (2005).
16. X. Shao, W. Zheng, and Z. Huang, "Polarized near-infrared autofluorescence imaging combined with near-infrared diffuse reflectance imaging for improving colonic cancer detection," Opt. Express **18**(23), 24293–24300 (2010).
17. M. G. Shim, L. M. Song, N. E. Marcon, and B. C. Wilson, "In vivo near-infrared Raman spectroscopy: demonstration of feasibility during clinical gastrointestinal endoscopy," Photochem. Photobiol. **72**(1), 146–150 (2000).
18. S. Duraipandian, M. Sylvest Bergholt, W. Zheng, K. Yu Ho, M. Teh, K. Guan Yeoh, J. Bok Yan So, A. Shabbir, and Z. Huang, "Real-time Raman spectroscopy for *in vivo*, online gastric cancer diagnosis during clinical endoscopic examination," J. Biomed. Opt. **17**(8), 081418 (2012).
19. G. A. Wagnières, W. M. Star, and B. C. Wilson, "In vivo fluorescence spectroscopy and imaging for oncological applications," Photochem. Photobiol. **68**(5), 603–632 (1998).
20. M. A. Mycek and B. W. Pogue, *Handbook of Biomedical Fluorescence* (Taylor & Francis, New York, 2003).
21. M. A. Mycek, K. T. Schomacker, and N. S. Nishioka, "Colonic polyp differentiation using time-resolved autofluorescence spectroscopy," Gastrointest. Endosc. **48**(4), 390–394 (1998).
22. L. Marcu, P. Butte, W. H. Yong, R. C. Thompson, K. L. Black, and B. Pikul, "Diagnosis of human brain tumor by lifetime fluorescence spectroscopy," in 23rd Annual Meeting of the American-Society-for-Laser-Medicine-and-Surgery, Surgical Applications (Lasers in Surgery and Medicine, 2003), p. 51.
23. L. Marcu, "Fluorescence lifetime techniques in medical applications," Ann. Biomed. Eng. **40**(2), 304–331 (2012).
24. N. Ramanujam, "Fluorescence spectroscopy of neoplastic and non-neoplastic tissues," Neoplasia **2**(1/2), 89–117 (2000).
25. P. A. A. De Beule, C. Dunsby, N. P. Galletly, G. W. Stamp, A. C. Chu, U. Anand, P. Anand, C. D. Benham, A. Naylor, and P. M. W. French, "A hyperspectral fluorescence lifetime probe for skin cancer diagnosis," Rev. Sci. Instrum. **78**(12), 123101 (2007).
26. A. J. Thompson, S. Coda, M. B. Sørensen, G. Kennedy, R. Patalay, U. Waitong-Brämming, P. A. A. De Beule, M. A. A. Neil, S. Andersson-Engels, N. Bendsøe, P. M. W. French, K. Svanberg, and C. Dunsby, "In vivo measurements of diffuse reflectance and time-resolved autofluorescence emission spectra of basal cell carcinomas," J. Biophotonics **5**(3), 240–254 (2012).
27. C. R. Kapadia, F. W. Cutruzzola, K. M. O'Brien, M. L. Stetz, R. Enriquez, and L. I. Deckelbaum, "Laser-induced fluorescence spectroscopy of human colonic mucosa. Detection of adenomatous transformation," Gastroenterology **99**(1), 150–157 (1990).
28. R. Richards-Kortum, R. P. Rava, R. E. Petras, M. Fitzmaurice, M. Sivak, and M. S. Feld, "Spectroscopic diagnosis of colonic dysplasia," Photochem. Photobiol. **53**(6), 777–786 (1991).
29. Y. Yang, G. C. Tang, M. Bessler, and R. R. Alfano, "Fluorescence spectroscopy as a photonic pathology method for detecting colon cancer," Lasers Life Sci. **6**, 259–276 (1995).
30. C. Eker, S. Montán, E. Jaramillo, K. Koizumi, C. Rubio, S. Andersson-Engels, K. Svanberg, S. Svanberg, and P. Slezak, "Clinical spectral characterisation of colonic mucosal lesions using autofluorescence and delta aminolevulinic acid sensitisation," Gut **44**(4), 511–518 (1999).
31. R. M. Cothren, R. Richards-Kortum, M. V. Sivak, Jr., M. Fitzmaurice, R. P. Rava, G. A. Boyce, M. Doxtader, R. Blackman, T. B. Ivanc, G. B. Hayes, M. S. Feld, and R. E. Petras, "Gastrointestinal tissue diagnosis by laser-induced fluorescence spectroscopy at endoscopy," Gastrointest. Endosc. **36**(2), 105–111 (1990).
32. K. T. Schomacker, J. K. Frisoli, C. C. Compton, T. J. Flotte, J. M. Richter, T. F. Deutsch, and N. S. Nishioka, "Ultraviolet laser-induced fluorescence of colonic polyps," Gastroenterology **102**(4 Pt 1), 1155–1160 (1992).

#194923 - $15.00 USD Received 31 Jul 2013; revised 11 Oct 2013; accepted 26 Nov 2013; published 16 Jan 2014

33. K. T. Schomacker, J. K. Frisoli, C. C. Compton, T. J. Flotte, J. M. Richter, N. S. Nishioka, and T. F. Deutsch, "Ultraviolet laser-induced fluorescence of colonic tissue: basic biology and diagnostic potential," Lasers Surg. Med. **12**(1), 63–78 (1992).
34. R. M. Cothren, M. V. Sivak, Jr., J. Van Dam, R. E. Petras, M. Fitzmaurice, J. M. Crawford, J. Wu, J. F. Brennan, R. P. Rava, R. Manoharan, and M. S. Feld, "Detection of dysplasia at colonoscopy using laser-induced fluorescence: a blinded study," Gastrointest. Endosc. **44**(2), 168–176 (1996).
35. B. Mayinger, P. Horner, M. Jordan, C. Gerlach, T. Horbach, W. Hohenberger, and E. G. Hahn, "Light-induced autofluorescence spectroscopy for tissue diagnosis of GI lesions," Gastrointest. Endosc. **52**(3), 395–400 (2000).
36. B. Mayinger, P. Horner, M. Jordan, C. Gerlach, T. Horbach, W. Hohenberger, and E. G. Hahn, "Light-induced autofluorescence spectroscopy for the endoscopic detection of esophageal cancer," Gastrointest. Endosc. **54**(2), 195–201 (2001).
37. B. Mayinger, M. Jordan, T. Horbach, P. Horner, C. Gerlach, S. Mueller, W. Hohenberger, and E. G. Hahn, "Evaluation of in vivo endoscopic autofluorescence spectroscopy in gastric cancer," Gastrointest. Endosc. **59**(2), 191–198 (2004).
38. B. W. Chwirot, S. Chwirot, W. Jedrzejczyk, M. Jackowski, A. M. Raczyńska, J. Winczakiewicz, and J. Dobber, "Ultraviolet laser-induced fluorescence of human stomach tissues: detection of cancer tissues by imaging techniques," Lasers Surg. Med. **21**(2), 149–158 (1997).
39. B. W. Chwirot, Z. Michniewicz, M. Kowalska, and J. Nussbeutel, "Detection of colonic malignant lesions by digital imaging of UV laser-induced autofluorescence," Photochem. Photobiol. **69**(3), 336–340 (1999).
40. S. D. Xiao, L. Zhong, H. Y. Luo, X. Y. Chen, and Y. Shi, "Autofluorescence imaging analysis of gastric cancer," Chin. Dig. Dis. **3**(3), 95–98 (2002).
41. B. Lin, S. Urayama, R. M. G. Saroufeem, D. L. Matthews, and S. G. Demos, "Real-time microscopic imaging of esophageal epithelial disease with autofluorescence under ultraviolet excitation," Opt. Express **17**(15), 12502–12509 (2009).
42. M. A. Kara, F. P. Peters, P. Fockens, F. J. ten Kate, and J. J. Bergman, "Endoscopic video-autofluorescence imaging followed by narrow band imaging for detecting early neoplasia in Barrett's esophagus," Gastrointest. Endosc. **64**(2), 176–185 (2006).
43. W. L. Curvers, R. Singh, L. M. Song, H. C. Wolfsen, K. Ragunath, K. Wang, M. B. Wallace, P. Fockens, and J. J. Bergman, "Endoscopic tri-modal imaging for detection of early neoplasia in Barrett's oesophagus: a multi-center feasibility study using high-resolution endoscopy, autofluorescence imaging and narrow band imaging incorporated in one endoscopy system," Gut **57**(2), 167–172 (2008).
44. T. Glanzmann, J. P. Ballini, H. van den Bergh, and G. Wagnieres, "Time-resolved spectrofluorometer for clinical tissue characterization during endoscopy," Rev. Sci. Instrum. **70**(10), 4067–4077 (1999).
45. J. D. Pitts and M. A. Mycek, "Design and development of a rapid acquisition laser-based fluorometer with simultaneous spectral and temporal resolution," Rev. Sci. Instrum. **72**(7), 3061–3072 (2001).
46. T. J. Pfefer, D. Y. Paithankar, J. M. Poneros, K. T. Schomacker, and N. S. Nishioka, "Temporally and spectrally resolved fluorescence spectroscopy for the detection of high grade dysplasia in Barrett's esophagus," Lasers Surg. Med. **32**(1), 10–16 (2003).
47. Q. Fang, T. Papaioannou, J. A. Jo, R. Vaitha, K. Shastry, and L. Marcu, "Time-domain laser-induced fluorescence spectroscopy apparatus for clinical diagnostics," Rev. Sci. Instrum. **75**(1), 151–162 (2004).
48. B. Li, Z. Zhang, and S. Xie, "Steady state and time-resolved autofluorescence studies of human colonic tissues," Chin. Opt. Lett. **4**, 348–350 (2006).
49. J. Mizeret, G. Wagnières, T. Stepinac, and H. Van Den Bergh, "Endoscopic tissue characterization by frequency-domain fluorescence lifetime imaging (FD-FLIM)," Lasers Med. Sci. **12**(3), 209–217 (1997).
50. J. McGinty, N. P. Galletly, C. Dunsby, I. Munro, D. S. Elson, J. Requejo-Isidro, P. Cohen, R. Ahmad, A. Forsyth, A. V. Thillainayagam, M. A. A. Neil, P. M. W. French, and G. W. Stamp, "Wide-field fluorescence lifetime imaging of cancer," Biomed. Opt. Express **1**(2), 627–640 (2010).
51. J. A. Jo, L. Marcu, Q. Fang, T. Papaioannou, J. H. Qiao, M. C. Fishbein, B. Beseth, A. H. Dorafshar, T. Reil, D. Baker, and J. Freischlag, "New methods for time-resolved fluorescence spectroscopy data analysis based on the Laguerre expansion technique--applications in tissue diagnosis," Methods Inf. Med. **46**(2), 206–211 (2007).
52. J. S. P. Lumley, J. L. Craven, and J. T. Aitken, *Essential Anatomy and Some Clinical Applications* (Churchill Livingstone, Edinburgh-New York 1995).
53. I. Georgakoudi, B. C. Jacobson, M. G. Müller, E. E. Sheets, K. Badizadegan, D. L. Carr-Locke, C. P. Crum, C. W. Boone, R. R. Dasari, J. Van Dam, and M. S. Feld, "NAD(P)H and collagen as in vivo quantitative fluorescent biomarkers of epithelial precancerous changes," Cancer Res. **62**(3), 682–687 (2002).
54. R. Drezek, K. Sokolov, U. Utzinger, I. Boiko, A. Malpica, M. Follen, and R. Richards-Kortum, "Understanding the contributions of NADH and collagen to cervical tissue fluorescence spectra: modeling, measurements, and implications," J. Biomed. Opt. **6**(4), 385–396 (2001).
55. S. Zhuo, J. Yan, G. Chen, J. Chen, Y. Liu, J. Lu, X. Zhu, X. Jiang, and S. Xie, "Label-free monitoring of colonic cancer progression using multiphoton microscopy," Biomed. Opt. Express **2**(3), 615–619 (2011).
56. M. Hilska, Y. Collan, J. Peltonen, R. Gullichsen, H. Paajanen, and M. Laato, "The distribution of collagen types I, III, and IV in normal and malignant colorectal mucosa," Eur. J. Surg. **164**(6), 457–464 (1998).
57. S. Zhuo, J. Yan, G. Chen, H. Shi, X. Zhu, J. Lu, J. Chen, and S. Xie, "Label-free imaging of basement membranes differentiates normal, precancerous, and cancerous colonic tissues by second-harmonic generation microscopy," PLoS ONE **7**(6), e38655 (2012).

#194923 - $15.00 USD Received 31 Jul 2013; revised 11 Oct 2013; accepted 26 Nov 2013; published 16 Jan 2014

58. L. Marcu, D. Cohen, J.-M. I. Maarek, and W. S. Grundfest, "Characterization of type I, II, III, IV, and V collagens by time-resolved laser-induced fluorescence spectroscopy," in Optical Biopsy III, (SPIE, 2000), 93–101.
59. J. M. Maarek, L. Marcu, W. J. Snyder, and W. S. Grundfest, "Time-resolved fluorescence spectra of arterial fluorescent compounds: reconstruction with the Laguerre expansion technique," Photochem. Photobiol. **71**(2), 178–187 (2000).
60. H. B. Manning, M. B. Nickdel, K. Yamamoto, J. L. Lagarto, D. J. Kelly, C. B. Talbot, G. Kennedy, J. Dudhia, J. Lever, C. Dunsby, P. French, and Y. Itoh, "Detection of cartilage matrix degradation by autofluorescence lifetime," Matrix Biol. **32**(1), 32–38 (2013).
61. H. D. Vishwasrao, A. A. Heikal, K. A. Kasischke, and W. W. Webb, "Conformational dependence of intracellular NADH on metabolic state revealed by associated fluorescence anisotropy," J. Biol. Chem. **280**(26), 25119–25126 (2005).
62. D. Chorvat, Jr. and A. Chorvatova, "Multi-wavelength fluorescence lifetime spectroscopy: a new approach to the study of endogenous fluorescence in living cells and tissues," Laser Phys. Lett. **6**(3), 175–193 (2009).
63. S. Zhuo, L. Zheng, J. Chen, S. Xie, X. Zhu, and X. Jiang, "Depth-cumulated epithelial redox ratio and stromal collagen quantity as quantitative intrinsic indicators for differentiating normal, inflammatory, and dysplastic epithelial tissues," Appl. Phys. Lett. **97**(17), 173701 (2010).
64. H. R. Williams, J. D. Willsmore, I. J. Cox, D. G. Walker, J. F. Cobbold, S. D. Taylor-Robinson, and T. R. Orchard, "Serum metabolic profiling in inflammatory bowel disease," Dig. Dis. Sci. **57**(8), 2157–2165 (2012).
65. S. Zhuo, J. Chen, G. Wu, S. Xie, L. Zheng, X. Jiang, and X. Zhu, "Quantitatively linking collagen alteration and epithelial tumor progression by second harmonic generation microscopy," Appl. Phys. Lett. **96**(21), 213704 (2010).
66. D. Schweitzer, S. Schenke, M. Hammer, F. Schweitzer, S. Jentsch, E. Birckner, W. Becker, and A. Bergmann, "Towards metabolic mapping of the human retina," Microsc. Res. Tech. **70**(5), 410–419 (2007).
67. S. Huang, A. A. Heikal, and W. W. Webb, "Two-photon fluorescence spectroscopy and microscopy of NAD(P)H and flavoprotein," Biophys. J. **82**(5), 2811–2825 (2002).
68. N. Nakashima, K. Yoshihara, F. Tanaka, and K. Yagi, "Picosecond fluorescence lifetime of the coenzyme of D-amino acid oxidase," J. Biol. Chem. **255**(11), 5261–5263 (1980).
69. M. C. Skala, K. M. Riching, A. Gendron-Fitzpatrick, J. Eickhoff, K. W. Eliceiri, J. G. White, and N. Ramanujam, "*In vivo* multiphoton microscopy of NADH and FAD redox states, fluorescence lifetimes, and cellular morphology in precancerous epithelia," Proc. Natl. Acad. Sci. U.S.A. **104**(49), 19494–19499 (2007).
70. L. Ludeman, R. M. Valori, and N. A. Shepherd, "The Principles and Techniques of Biopsy: With Special Reference to Endoscopic Biopsy," Surgery **20**, iii–vii (2002) (Medicine Publishing).
71. G. M. Palmer, C. L. Marshek, K. M. Vrotsos, and N. Ramanujam, "Optimal methods for fluorescence and diffuse reflectance measurements of tissue biopsy samples," Lasers Surg. Med. **30**(3), 191–200 (2002).
72. J. A. Palero, A. N. Bader, H. S. de Bruijn, A. der Ploeg van den Heuvel, H. J. Sterenborg, and H. C. Gerritsen, "In vivo monitoring of protein-bound and free NADH during ischemia by nonlinear spectral imaging microscopy," Biomed. Opt. Express **2**(5), 1030–1039 (2011).

1. Introduction

Neoplasms of the gastrointestinal (GI) tract account for approximately a quarter of worldwide cancer mortality, equivalent to an incidence of about 2 million new cases each year [1, 2]. Prevention is based on early detection and excision of premalignant lesions (e.g. dysplasia, adenomas) and early stage cancers during endoscopic examination. This significantly increases patient survival while reducing disease progression and direct medical costs [3]. However, early stage lesions are often invisible or difficult to visualize under inspection with white light endoscopy (WLE) alone. In addition, it is often difficult to distinguish between benign and early or premalignant lesions, such as between inflammatory disorders and adenomas. This difficulty is currently overcome through taking a tissue biopsy specimen that is subsequently processed and assessed by a histopathologist. Neoplastic polyps are of particular clinical significance because of their established role in the stepwise process that results in colorectal cancer (the adenoma-carcinoma sequence) [4]. However, macroscopic discrimination between neoplastic polyps (consisting of adenomas with low grade or high grade dysplasia, and carcinomas) and non-neoplastic polyps (e.g. hyperplastic, inflammatory pseudopolyps, hamartomas) during WLE is extremely difficult. Therefore all polyps are removed when detected unless there is a clinical reason to delay the endoscopic resection and, following the current clinical best practice in GI endoscopy for tissue abnormalities, are biopsied or excised and sent for histological assessment and interpretation. This leads to unnecessary removal of benign lesions and a considerable number of tissue biopsies, which

#194923 - $15.00 USD Received 31 Jul 2013; revised 11 Oct 2013; accepted 26 Nov 2013; published 16 Jan 2014

are a significant burden on the healthcare system [5] and can be coupled with a low diagnostic yield [6, 7].

A non-invasive method of diagnosis could remove the need for physical biopsy and provide improvements in diagnostic accuracy for a number of diseases. Although several novel imaging techniques that can be operated in conjunction with standard WLE have recently become available in the clinical setting – such as narrow-band imaging (NBI) [8], autofluorescence imaging (AFI) [9] and more recently confocal endomicroscopy (CLE) [10, 11] – there is still no red flag technique for detection of GI premalignant lesions that can progress into cancer. Furthermore, there is currently no technology that can reliably indicate when it is appropriate not to biopsy. As a result, despite the use of advanced imaging, in most cases multiple biopsies are still required to confirm or reject the endoscopic diagnosis.

Various other optical approaches are being investigated for their potential to provide an *in vivo* label-free "optical biopsy" to aid diagnosis of GI disease, with the ultimate aim of allowing clinicians to avoid multiple unnecessary and/or random biopsies and instead permit targeting of both biopsies and resections. These include point probe-based diffuse reflectance spectroscopy [12–14], which has been applied to *in vivo* detection of dysplasia in Barrett's esophagus (BE) [15] and to *ex vivo* surgical specimens of colon cancer [16], and Raman spectroscopy [17], which has recently been applied in a large study of 305 patients [18]. In this work we chose to focus on autofluorescence (AF) spectroscopy and lifetime measurements as they can be extended from point-based measurements to wide-field imaging once the spectroscopic features presenting the greatest contrast between normal and diseased tissue have been identified.

Tissue autofluorescence arises from intracellular and extracellular endogenous fluorophores, such as collagen, elastin, pyridine nucleotides and flavins. The fluorescence signatures of these substances – along with their local distributions – have the ability to report on tissue disease state [19]. Further information can be obtained from the autofluorescence excitation and emission spectra [19, 20] and the decay rate (or fluorescence lifetime) [21–26].

A number of previous studies have investigated differences in autofluorescence emission spectra between healthy and diseased colonic tissue. Such investigations have demonstrated contrast in a variety of tissue types including: between normal tissue and adenomatous (i.e. neoplastic) polyps *ex vivo* [27–29]; between normal tissue and adenomas *in vivo* [30]; between normal tissue or hyperplastic polyps and adenomas [31]; between hyperplastic polyps and adenomas [32, 33]; and between all three of the above tissue groups [34]. Cancers in the upper GI tract (esophagus and stomach) have also been investigated [35–37]. In addition to point measurements of autofluorescence emission spectra, there have also been a number of applications of AFI modalities to the study of GI tissue [38–41]. AFI has been combined with high-definition videoendoscopy (HDE) [42] and also with NBI in so-called "trimodal imaging", which has been applied to the study of Barrett's neoplasia [43]. However, none of the currently available techniques has been able to provide a clinical red flag technique for rapid and reliable detection of early changes of disease and it is interesting to investigate further sources of spectroscopic contrast such as autofluorescence lifetime (AFL). Ideally such a clinical technique should be able to survey wide areas of tissue for screening as well as offering the ability to obtain detailed information at specific points of interest.

Time-resolved point-probe spectroscopy instrumentation has been developed by a number of groups [21, 44–47]. Time-resolved autofluorescence spectroscopy in the GI tract was pioneered by Mycek *et al.*, whose *in vivo* study [21] on 24 polyps (13 adenomas, 11 non-adenomas) from 17 patients using an excitation wavelength of 337 nm and detection in the range 530-570 nm demonstrated shorter average lifetimes for neoplastic polyps (adenomas) compared to non-neoplastic polyps (9300 ± 400 ps vs. 10500 ± 700 ps). In work by Li *et al*. in *ex vivo* tissue, longer AF lifetimes were found in cancerous colonic tissues using excitation at 397 nm and detecting at 635 nm compared to normal colon (18,450 vs. 4320 ps). This was attributed to the contribution of protoporphyrin IX (PpIX), which is known to both

#194923 - $15.00 USD Received 31 Jul 2013; revised 11 Oct 2013; accepted 26 Nov 2013; published 16 Jan 2014

accumulate in neoplasia and to have a long fluorescence lifetime [48]. Pfefer *et al*. [46] used excitation wavelengths of 337 and 400 nm and compared measurements of fluorescence emission spectra and fluorescence decay profiles acquired at 550 nm *in vivo* in 37 patients undergoing routine endoscopic surveillance for BE. In this study time-resolved fluorescence was unable to achieve sensitivity and specificity values above 60% for discriminating high risk (carcinoma, high grade dysplasia) from low risk (low grade dysplasia, non-dysplastic or indefinite for dysplasia) tissue, while moderate overall accuracy was achieved using steady-state fluorescence only.

To date, fluorescence lifetime imaging (FLIM) has only been applied to *ex vivo* studies of GI tissue. Mizeret *et al*. reported an increased fluorescence lifetime of an *ex vivo* human oral carcinoma compared to its surrounding uninvolved tissue [49] using frequency domain FLIM with 417 nm excitation with an argon ion laser-pumped dye laser and an emission detection band from 470 nm to 650 nm. Subsequently a more extensive study utilizing wide-field time-gated FLIM with 355 nm excitation from a frequency-tripled Nd:YVO_4 laser demonstrated a statistically significant increase in the fluorescence lifetime of invasive colonic adenocarcinomas (16 specimens) relative to the surrounding healthy tissue, while a decrease in fluorescence lifetime was observed in two serrated adenomas with focal high grade dysplasia [50].

The studies outlined above have motivated us to develop and evaluate instrumentation exploiting spectral and lifetime readouts of autofluorescence to contrast healthy and diseased GI tissue autofluorescence, in particular for colonic polyps. We have worked to develop compact and portable instrumentation utilizing picosecond gain-switched diode lasers operating at 20 MHz and are particularly interested to compare autofluorescence readouts with ultraviolet (375 nm) and blue (435 nm) excitation, noting the advantages of lower photodamage/phototoxicity, instrument background fluorescence and attenuation for longer wavelength excitation. In this study we are using point spectroscopy and integrating all spatial information to provide spectral and temporal resolution to higher precision than is practical when imaging. The resulting clinical spectroscopic data will then be used to guide the development of new clinical FLIM-based endoscopes intended to rapidly screen large areas of GI tissue. Here we describe a clinical study of colonic tissue that has been freshly biopsied/resected from patients undergoing endoscopy using a fiber-optic probe-based instrument with excitation at 375 nm and 435 nm and detection of the autofluorescence using a time-resolved fluorescence spectrometer.

2. Materials and methods

2.1 Patient enrolment

A total of 47 endoscopic samples from different regions of colon were collected from 17 patients undergoing colonoscopy. Each of these samples was then studied with the point-probe system described below. All samples were submitted for histopathology following the optical measurements. Normal tissue, colonic polyps and inflammatory bowel disease (IBD) were investigated.

Patients who participated in the research were recruited by the clinical team and gave their informed consent to participate. The study was carried out with the approval of the National Research Ethics Service (REC reference number 09/H0706/28).

2.3 Fluorescence lifetime spectroscopy (FLS) instrumentation

The optical system, which is represented in Fig. 1, is similar to that described in references [25, 26] but has been adapted for clinical deployment. Two pulsed diode lasers were used as excitation sources with central emission wavelengths of 375 nm and 435 nm (LDH-P-C-375B and LDH-P-C-440B respectively, PicoQuant GmbH, Germany). Both lasers emit pulses of 50-150 ps duration and were configured to operate at 20 MHz. The outputs from the two

#194923 - $15.00 USD Received 31 Jul 2013; revised 11 Oct 2013; accepted 26 Nov 2013; published 16 Jan 2014

lasers were first combined and then coupled into the fluorescence excitation channel of a custom-built optical fiber probe (FiberTech Optica, Canada). This custom fiber probe comprised 19 multimode optical fibers (all of 0.22 NA and 200 μm diameter), of which 3 were used to deliver the laser excitation to the sample and 14 were used to collect the resulting fluorescence. Two fibers in the bundle were unused.

The distal branch of the probe (common to all optical fibers) was 3 m in length. At the distal end of the probe the fibers were arranged as shown in the lower central inset of Fig. 1. A medical grade stainless steel distal ferrule – protruding in front of the fiber output face – ensured that the sample was kept at a fixed distance of 1.5 mm from the distal face of the fiber bundle. This resulted in the excitation lasers illuminating an area of tissue of approximately 0.9 mm^2. A neutral density (ND 0.7) filter was placed in the path of the 375 nm laser in order to limit the average optical power at the sample to 35 μW. A bandpass filter (Z440/20x, Chroma Technology, USA) was used to narrow the spectrum of the 435 nm laser, which provided a maximum average power of 200 μW at the sample. The outputs of the two laser sources were controlled via computer and used to illuminate the specimen sequentially. In the investigation presented here, each measurement consisted of 5 s fluorescence data acquisition with the 375 nm laser followed by 5 s of acquisition with the 435 nm laser. This cycle was repeated 3 times and the total acquisition time was approximately 35 s.

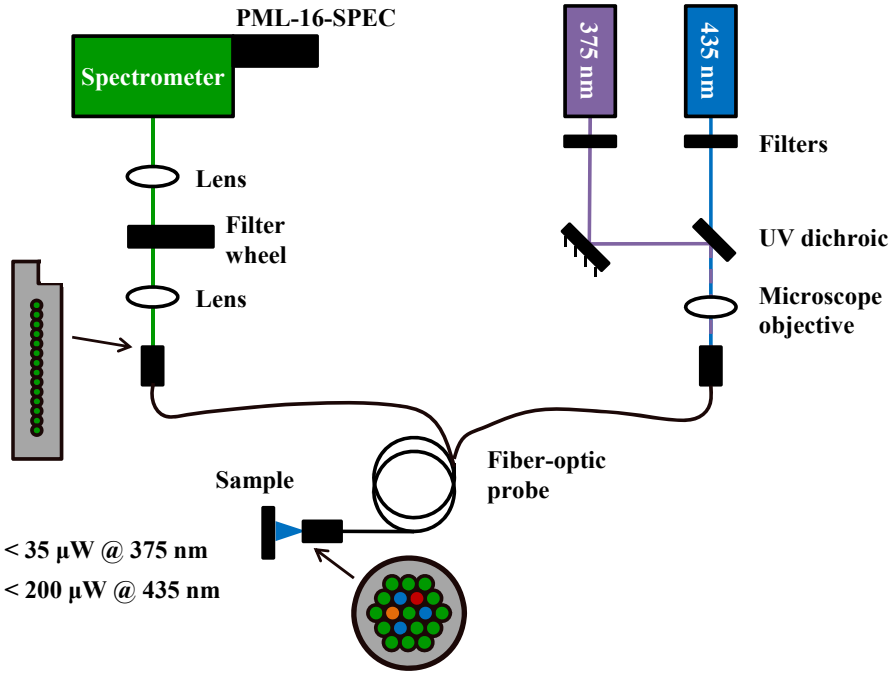

Fig. 1. Optical configuration of the fiber-optic probe-based fluorescence lifetime spectroscopy system. Insets show the arrangement of the optical fibers in the custom fiber bundle at the distal end of the probe and at the output of the fluorescence detection branch of the proximal end of the probe. Cores shown in green are fluorescence detection fibers; fibers colored blue are used to deliver the laser excitation; the orange and red cores were unused in this study.

The resulting fluorescence was collected by the 14 fluorescence detection fibers that relay the collected light to the fluorescence detection arm of the spectrofluorometer (left hand side of Fig. 1). The output from the collection fibers is imaged onto the input slit of a grating spectrometer (MS125 1/8m, Lot-Oriel, UK), which is attached to a 16 channel multi-anode photomultiplier tube (PMT) detector (PML-16-SPEC, Becker-Hickl GmbH, Germany). The

#194923 - $15.00 USD Received 31 Jul 2013; revised 11 Oct 2013; accepted 26 Nov 2013; published 16 Jan 2014

PMT was linked to a computer with a time correlated single photon counting (TCSPC) card (SPC-730, Becker-Hickl, GmbH, Germany) and this allowed collection of fluorescence decays in 16 spectral channels spanning a wavelength range of 400-600 nm. At the fiber probe output, the 14 collection fibers were aligned vertically in order to maximize the coupling into the input slit of the spectrograph (see inset on left of Fig. 1). A motorized filter wheel was placed between the fiber probe output and the grating spectrometer. This filter wheel contained two emission filters, E400LPv2 and E475LPv2 (Chroma Technology, USA), that were used in combination with the 375 and 435 nm excitation lasers respectively to ensure that no scattered laser radiation reached the PMT detector. All optical components were mounted on a 30 × 45 cm^2 breadboard, and the breadboard and all electrical components were housed and enclosed within a compact (182 × 70 × 55 cm^3) wheeled trolley. The entire system is controlled through software written in LabVIEW 7.1 (National Instruments, USA). The optical fiber was designed such that it can be sterilized for future *in vivo* clinical measurements.

In order to analyze the raw fluorescence data it was necessary to determine the wavelength range collected by each PMT element and to determine its relative sensitivity. This was performed in an identical manner to that described in references [25, 26]. First, the distal end of the fiber probe was illuminated with white light passed through a calibrated monochromator, which allowed the spectral center and bandwidth of each detection channel to be determined. Second, the relative sensitivity of each PMT element was found by recording the emission from a calibrated white light source (LS-1-CAL, Ocean Optics, The Netherlands) and this information was then used to correct the fluorescence intensity measured in each spectral channel.

2.4 Experimental procedure

During routine clinical endoscopy, pinch biopsy samples of any suspicious regions of tissue were taken with 'jumbo' biopsy forceps (Radial Jaw 3 LC forceps, Boston Scientific) and any superficial lesions (i.e. polyps) were removed with either a cold or a hot snare (Captivator single-use snares, Boston Scientific) according to standard practice in patient care. Polyps removed by hot snare polypectomy were sufficiently large (4-15 mm in diameter) that the area measured using the optical system was unaffected by any specimen heating. Where clinically possible, at least one biopsy of healthy tissue was also taken from each patient with a suspicious region and the healthy biopsy was taken as close as possible to the suspicious region. After completion of an endoscopic examination, any tissue samples obtained were immediately delivered to the adjacent spectroscopy room and measured with the fluorescence lifetime spectroscopy (FLS) system.

All samples were measured within approximately 10 minutes of excision. Once removed, the biopsy samples or excised polyps were carefully teased onto gauze with sterile disposable tweezers, keeping the mucosal surface facing upward. All samples were washed gently by dripping Hanks' Balanced Salt Solution (HBSS) onto them. The distal tip of the optical fiber probe was then placed *en face* in contact with the sample and data acquisition was performed as described in the previous section. To ensure that the sample was not damaged by mechanical stress and to simulate *in vivo* probing, the distal end of the probe was held by hand, exerting constant gentle pressure throughout the measurements. There were no visible changes in the texture or appearance of the samples over the duration of the measurements and the sample thickness always remained consistent (compared to the original condition). Following measurements with the FLS system, all tissue samples were sent for histopathology where hematoxylin and eosin (H&E) stained tissue sections were reviewed by an experienced histopathologist (GWS). Each sample was assigned a unique number for identification purposes and the characteristics of the specimens investigated in this study are summarized in Table 1.

#194923 - $15.00 USD Received 31 Jul 2013; revised 11 Oct 2013; accepted 26 Nov 2013; published 16 Jan 2014

Table 1. Summary showing the clinical diagnoses of all the *ex vivo* samples investigated with the endoscopic spectrometer

Tissue type		**Number of samples**
Endoscopic diagnosis	Histological diagnosis	
Colonic polyps	12x tubular adenomas with LGD	22
	2x mixed hyperplastic adenomatous polyp with LGD	
	2x hyperplastic polyp	
	1x serrated polyp	
	3x inflammatory polyp	
	1x nonspecific reactive changes	
	1x normal colonic mucosa	
IBD	1x active chronic inflammation	6
	2x severe chronic ulcerative colitis	
	2x moderate chronic colitis	
	1x basal inflammation	
Total number of diseased tissue measurements		28
Normal colon tissue	18x normal colonic mucosa	19
	1x active chronic inflammation	
Total number of measurements		47

LGD, low grade dysplasia; IBD, inflammatory bowel disease.

3. Data analysis

3.1 Exponential fitting of autofluorescence decay profiles

Autofluorescence from biological tissue typically exhibits a complex exponential decay profile as tissue contains several fluorescent species, each with a number of possible states (e.g. oxidized/reduced and free/protein bound). Thus, it is common practice to fit a multi-exponential decay model to the recorded tissue fluorescence data. With an average of 2×10^5 photons collected in each spectrally resolved decay profile, we chose to fit to a double exponential model given by Eq. (1), where τ_1 and τ_2 are the two lifetimes, and a_1 and a_2 are two pre-exponential amplitudes.

$$I(t) = a_1 \exp\left(\frac{-t}{\tau_1}\right) + a_2 \exp\left(\frac{-t}{\tau_2}\right) \quad (1)$$

The average reduced chi-squared produced by this fit model was 1.3 for 375 nm excitation and 2.6 for 435 nm excitation indicating that this model provides a reasonable fit to the data. More complex decay models, e.g. a triple exponential decay model, would provide better fits and lower reduced chi-squared values and have previously been used when analyzing lifetime data of biological tissue AF. However, the improved fit is often only the result of the higher number of fitting parameters used and it is no more realistic to assume the presence of 3 mono-exponentially decaying fluorophores (or a single fluorophore with 3 discrete decay constants) than it is to assume the presence of one or two fluorophores. Because fitting three

#194923 - $15.00 USD Received 31 Jul 2013; revised 11 Oct 2013; accepted 26 Nov 2013; published 16 Jan 2014

or more exponential decays is more vulnerable to noise artifacts and requires a significantly greater number of detected photons than we were able to collect, we believe that using a double exponential decay model to parameterize the AF decay curves is a useful approach to investigate for contrast between different tissues. Other arbitrary complex models, e.g. based on Laguerre polynomial fits [51] could also provide empirically useful data.

Reflected light temporal instrument response functions (IRFs) were recorded for each PMT channel by placing a diffusely reflecting sample at a short distance (~10 cm) from the distal end of the point-probe and then adjusting the angle of the grating in the spectrometer to direct light onto each PMT element in sequence. To account for the temporal shift of the IRF with respect to the data, a temporal offset fit parameter was included in the fluorescence decay analysis.

3.2 Fluorescence data analysis

Having fitted the fluorescence decay profiles according to Eq. (1), we calculated the mean fluorescence lifetime (τ_{mean}) in each spectral channel. This was achieved as shown in Eq. (2).

$$\tau_{mean} = \frac{a_1\tau_1^2 + a_2\tau_2^2}{a_1\tau_1 + a_2\tau_2} \tag{2}$$

For each measurement, the variation in the mean lifetime was investigated as a function of emission wavelength. To summarize the fluorescence lifetime data from each sample in a simple manner, we then calculated a spectrally-averaged fluorescence lifetime for each measurement by averaging the spectrally resolved mean lifetime values and weighting the data according to the fluorescence intensity observed in each channel, as described by Eq. (3).

$$\overline{\tau}_{spectral} = \frac{\sum_{i=1}^{n} I_i\tau_i}{\sum_{i=1}^{n} I_i} \tag{3}$$

Here, $\overline{\tau}_{spectral}$ is the spectrally averaged mean lifetime, n is the number of spectral channels included in the average and I_i and τ_i are respectively the total number of photons and mean lifetime recorded in each of the spectral detection channels. For 375 nm excitation, the spectrally averaged mean lifetime was calculated over the range 418-582 nm, excluding the first and last spectral channels owing to the weak signal and poor decay fitting in these channels. For 435 nm excitation, the spectrally averaged mean lifetime was calculated over channels 7-15 (481-582 nm) for the same reason. Following the initial analysis, we observed that the greatest lifetime contrast with 375 nm excitation for IBD was observed in spectral channels 8-13 (494-556 nm) and we therefore calculated a 2nd spectrally averaged mean lifetime over this narrower range.

For each lesion, the difference between its spectrally averaged mean lifetime and that of a neighboring healthy tissue sample (excised from the same patient) was calculated (i.e. $\Delta\tau = \tau_{lesion} - \tau_{normal}$) in order to investigate the diagnostic potential of the fluorescence lifetime data, noting that this paired analysis of the fluorescence lifetime avoids the impact of inter-patient variation in the fluorescence lifetimes measured for normal tissue. The spectral properties of the samples were also investigated using their fluorescence emission spectra where the area under the fluorescence emission spectrum was normalized to unity. The mean fluorescence emission wavelength was also calculated for each sample and for each excitation wavelength. Finally, Wilcoxon signed rank tests were performed on all sets of spectrally averaged lifetime or mean emission wavelength shifts in order to test for statistically significant differences between healthy and diseased tissue. In all cases, the null hypothesis

#194923 - $15.00 USD Received 31 Jul 2013; revised 11 Oct 2013; accepted 26 Nov 2013; published 16 Jan 2014

being tested was that the measured lifetime or wavelength shifts come from a continuous, symmetric distribution with zero median.

4. Results

The analysis was performed using the histological diagnosis for each sample as the gold standard. Samples were excluded if microscopic analysis revealed normal large bowel mucosa in clinically abnormal samples or histological abnormalities in clinically normal specimens.

4.1 Normal tissue characterization

In the first part of our study we investigated the measured fluorescence emission spectra and fluorescence lifetimes in histologically normal tissue. Figures 2(a) and 2(b) show exemplar histological H&E stained sections of normal colon from a patient diagnosed with a polyp (a) and IBD (b), where a regular crypt architecture can be seen, including numerous mucin rich goblet cells assorted around the inner rim of the crypt openings (green arrowheads). Figures 2(c) and 2(d) show the mean fluorescence emission spectra from histologically normal colon obtained from patients diagnosed with a polyp or IBD. Normal colon from patients with IBD shows a slight shift to shorter emission wavelengths for 375 nm excitation compared to normal colon obtained from patients diagnosed with a polyp. There is also a slight shift to longer emission wavelengths for excitation at 435 nm. However, the change in mean emission wavelength was not found to be statistically significant for either excitation wavelength. The fluorescence lifetime recorded in each spectral channel for normal tissue from patients diagnosed with a polyp and IBD is plotted in Figs. 2(e) and 2(f). For 375 nm excitation, the mean fluorescence lifetime varies slightly with emission wavelength, with a maximum at an emission wavelength of around 500 nm. For 435 nm excitation, the mean fluorescence lifetime is more consistent with emission wavelength. In order to get a better overview of the fluorescence lifetime, we calculated the spectrally averaged fluorescence lifetimes – see Fig. 2(g) – which shows that there is a higher mean fluorescence lifetime for normal tissue with 435 nm excitation for patients diagnosed with a polyp compared to patients diagnosed with IBD. However, this shift was not found to be statistically significant by two-way ANOVA (normal data was tested according to both diagnosis ($p = 0.11$) and region ($p = 0.30$), null hypothesis that all groups are drawn from populations with the same mean).

#194923 - $15.00 USD Received 31 Jul 2013; revised 11 Oct 2013; accepted 26 Nov 2013; published 16 Jan 2014

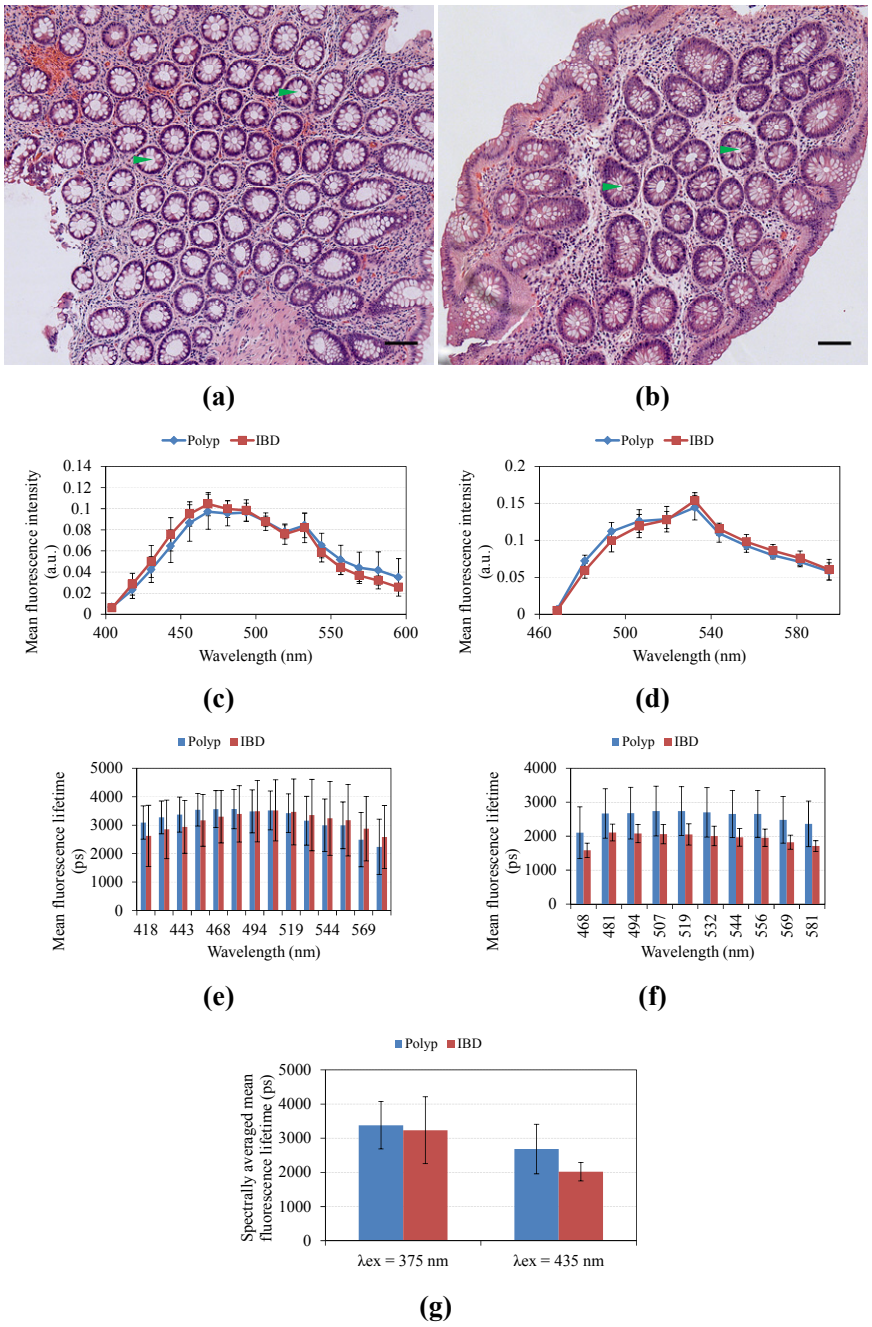

Fig. 2. Summary of results from normal tissues grouped according to whether the patient was diagnosed with a polyp (n = 13) or IBD (n = 4). (a & b) Exemplar H&E stained histological sections of a biopsy sample of normal colon from a patient diagnosed with a polyp (a) and IBD (b). Scale bar represents 100 μm, see text for description of arrowheads. (c) & (d) show the mean fluorescence emission spectra obtained with 375 and 435 nm excitation, respectively. (e) & (f) show the spectrally resolved fluorescence lifetimes for 375 and 435 nm excitation, respectively. (g) shows the spectrally averaged mean fluorescence lifetimes for both groups and for both excitation wavelengths. The error bars represent ± 1 standard deviation in all panels.

#194923 - $15.00 USD Received 31 Jul 2013; revised 11 Oct 2013; accepted 26 Nov 2013; published 16 Jan 2014

We also grouped the fluorescence lifetime data from all histologically normal samples according to the region of colon from which they were obtained. Figures 3(a) and 3(b) show a slight blue shift in the fluorescence emission spectrum for the two specimens obtained from the rectum for 375 nm excitation, but this shift in mean emission wavelength was not found to be significant by 2-way ANOVA (grouping data by both diagnosis and region) for either excitation wavelength.

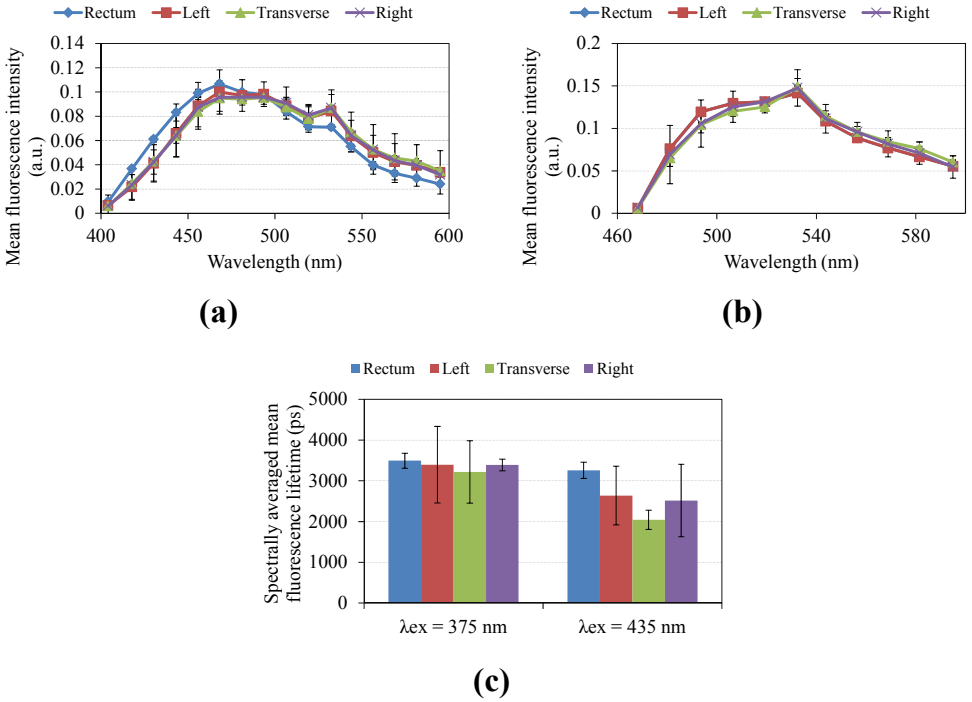

Fig. 3. Summary of results from normal tissues grouped according to the location that the specimen was taken from. The number of specimens in each group was: rectum (n = 2), left (n = 8), transverse (n = 5), right (n = 3). (a) & (b) show the mean fluorescence emission spectra obtained with 375 and 435 nm excitation respectively. (c) shows the spectrally averaged mean fluorescence lifetimes for both groups and for both excitation wavelengths. The error bars represent ± 1 standard deviation in all panels.

The mean fluorescence lifetime obtained with 435 nm excitation from the two rectal specimens is longer than that obtained from the other three regions; see Fig. 3(c). As reported above, however, we performed 2-way ANOVA on the spectrally averaged mean fluorescence lifetimes from histologically normal colon grouped according to both diagnosis and region of colon and no statistically significant differences were obtained.

4.2 Diseased vs. normal tissue

Of the 22 clinically identified polyps (see Table 1), one was excluded as it was found to be normal by histopathology. The polyp specimens included in our analysis are summarized in Table 2. Where possible, at least one specimen of normal colon was obtained from all patients.

4.2.1 Colonic polyps

Figures 4(a) and 4(b) show exemplar histological H&E stained sections of (a) neoplastic and (b) non-neoplastic polyps, respectively. In neoplastic tissue (adenomatous polyp), the crypts appear displaced by large dense branching bands of interstitial space mostly free of cells.

#194923 - $15.00 USD Received 31 Jul 2013; revised 11 Oct 2013; accepted 26 Nov 2013; published 16 Jan 2014

Crypts are distorted and elongated (red asterisks), and significantly fewer goblet cells can be observed, which are now replaced by crowded elongated cells with large nuclei (red arrowheads). In non-neoplastic tissue (hyperplastic polyp), glands have a star-shaped lumen (green asterisks) – when seen in cross-sections – that is characteristic of these polyps. Crypts are straight, narrowed and hyperchromatic at the base. Nuclei are small, regular, round and with basal orientation with respect to the crypt lumen (green arrowheads) and dysplastic changes are not present. The basal membrane is also commonly thickened.

Figures 4(c) and 4(d) show the normalized mean fluorescence spectra observed in normal colon tissue and in neoplastic (tubular adenomas with LGD and mixed hyperplastic adenomatous polyps) and non-neoplastic (hyperplastic and inflammatory) colonic polyps for both excitation wavelengths. These spectra overlap within the error bars and no statistically significant difference was obtained when comparing the mean fluorescence emission wavelength for either excitation wavelength. Figures 4(e) and 4(f) show the mean fluorescence lifetimes measured in each spectral channel for both 375 and 435 nm excitation. The mean fluorescence lifetimes for neoplastic polyps were shorter than those observed in normal tissue for both excitation wavelengths and this trend was observed in all spectral channels. The spectrally averaged mean fluorescence lifetime (weighted according to the intensity recorded in each spectral channel) for normal tissue, neoplastic and non-neoplastic polyps is shown in Fig. 4(g).

As can be seen from the size of the error bars on the fluorescence lifetime measurements in Fig. 4, there is significant inter-patient variability in the measured mean fluorescence lifetime from both normal and diseased specimens. Therefore, in order to overcome this variability, we conducted a paired analysis by calculating the difference in spectrally averaged mean fluorescence lifetime between normal and lesional specimens obtained from the same patient. This paired analysis was performed using a total of 30 specimens (see Table 2).

#194923 - $15.00 USD Received 31 Jul 2013; revised 11 Oct 2013; accepted 26 Nov 2013; published 16 Jan 2014

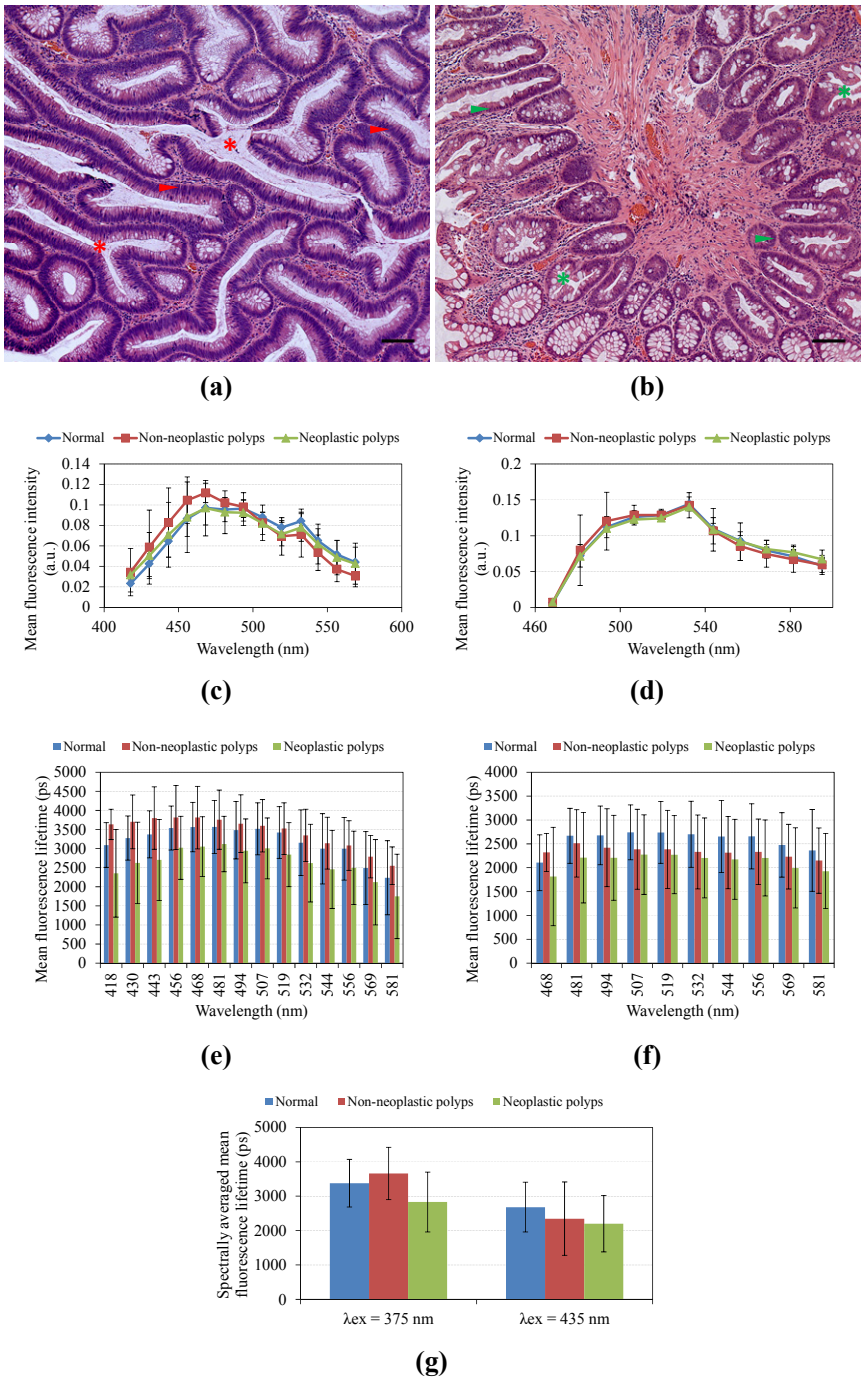

Fig. 4. Comparison of normal tissue versus neoplastic and non-neoplastic polyp specimens. (a) & (b) show exemplar H&E stained histological sections of (a) neoplastic (adenomatous polyp) and (b) non-neoplastic (hyperplastic polyp) polyps, respectively. Scale bar represents 100 μm, see text for description of arrowheads and asterisks. (c) & (d) show the mean fluorescence emission spectra obtained with 375 and 435 nm excitation, respectively. (e) & (f) show the spectrally resolved fluorescence lifetimes with 375 and 435 nm excitation, respectively. (g) shows the spectrally averaged mean fluorescence lifetimes for all three groups and for both excitation wavelengths. The error bars represent ± 1 standard deviation in all panels.

#194923 - $15.00 USD Received 31 Jul 2013; revised 11 Oct 2013; accepted 26 Nov 2013; published 16 Jan 2014

Table 2. Summary of colonic polyps included in study

	Unpaired analysis	Paired analysis
No. of patients	12	11
No. of polyps	21	18
Neoplastic	15	12
Non-neoplastic	6	6
No. of normal specimens	13	12

Three polyps obtained from one patient were excluded from the paired analysis as it was not clinically possible to obtain a normal specimen in this patient. In the one patient where two normal specimens were obtained, the lesional specimens were compared to the anatomically closest normal specimen.

For each normal-lesion pair, both the shift in mean fluorescence emission wavelength and the shift in spectrally averaged mean fluorescence lifetime were calculated for both excitation wavelengths. The measured shift in mean fluorescence emission wavelength was not found to be statistically significant for either excitation wavelength. Figure 5 shows the shift in the spectrally averaged fluorescence lifetime ($\Delta\tau$) for each normal-lesion pair. The mean values calculated over all pairs for neoplastic polyps and non-neoplastic polyps are summarized in Table 3.

Table 3. Spectrally averaged fluorescence lifetime shift for neoplastic and non-neoplastic polyps

	Mean shift in spectrally averaged fluorescence lifetime of polyp compared to normal tissue from same or nearest region of colon (ps)		Mean shift in spectrally averaged fluorescence lifetime of polyp compared to normal tissue from same region of colon (ps)	
Excitation wavelength	375 nm	435 nm	375 nm	435 nm
Neoplastic	**-230 ± 560**	**-570 ± 740**	**-310 ± 510**	**-690 ± 640**
		(p = 0.021)		**(p = 0.0049)**
Non-neoplastic	25 ± 820	−160 ± 780	−250 ± 680	−620 ± 400

A Wilcoxon signed rank test was applied to all sets of paired difference values. The data obtained with 375 nm excitation showed no significant differences while the 435 nm excited data shows a statistically significant decrease in the fluorescence lifetime of neoplastic polyps with respect to healthy tissue (p = 0.021). We also found that the spectrally averaged difference in τ_2 between neoplastic polyp and normal tissue for 435 nm excitation was statistically significant ($\Delta\tau_2$ = −690 ± 970 ps, p = 0.05). The difference in spectrally averaged mean lifetime shift between neoplastic and non-neoplastic polyps for 435 nm excitation was not found to be statistically significant (Wilcoxon rank sum test).

#194923 - $15.00 USD Received 31 Jul 2013; revised 11 Oct 2013; accepted 26 Nov 2013; published 16 Jan 2014

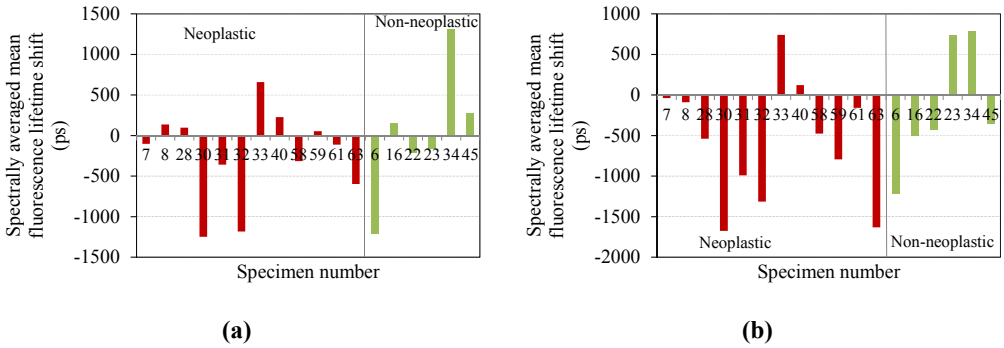

Fig. 5. Shift in the spectrally averaged mean fluorescence lifetime for (a) 375 nm and (b) 435 nm excitation of neoplastic (red) and non-neoplastic polyp (green) specimens. Lifetime shifts are calculated using a measurement of normal tissue obtained from the same or nearest region of colon (paired analysis).

Specimens 23, 33 and 34 correspond to patients where the normal sample was not taken from the same region of colon as the polyp. If these specimens are excluded from the analysis then for 435 nm excitation the shift in mean emission wavelength averaged over all neoplastic specimen pairs becomes 2.6 ± 3.1 nm ($p = 0.019$) and the shift in spectrally averaged mean lifetime averaged over all neoplastic specimen pairs becomes –690 ± 640 ps ($p = 0.0049$), see Table 3. The increase in mean emission wavelength at this excitation wavelength was found to be correlated with the decrease in fluorescence lifetime ($R^2 = 0.71$). While the shift in spectrally averaged 435 nm excited mean fluorescence lifetime for non-neoplastic polyps decreased, it was not found to be statistically significant.

4.2.2 Inflammatory bowel disease

A total of 11 specimens (6 diseased and 5 normal) were measured from 5 patients with IBD. One normal and one IBD specimen (from different patients) were excluded because the histopathological assessment revealed no difference between the normal and the diseased samples. Therefore, we analyzed the numbers of specimens shown in Table 4.

Table 4. Summary of IBD (inflammatory bowel disease) specimens included in the study, divided by type of analysis performed

	Unpaired analysis	Paired analysis
No. of patients	5	3
No. of IBD specimens	5	4
No. of normal specimens	4	3
Total No. of specimens	9	7

Figures 6(a) and 6(b) show exemplar histological H&E stained sections of (a) normal colonic mucosa and (b) IBD tissue, respectively. Both samples were taken from the same patient affected by active distal ulcerative colitis. Regular crypt architecture can be seen in the uninflamed mucosa (Fig. 6(a)). In contrast, moderate chronic active inflammation with severe distortion of crypt architecture and prominent crypt abscesses with disruption of crypts and areas of crypt loss is observed in the inflamed tissue (red arrowheads in Fig. 6(b)). Goblet cell and mucin depletion with reactive atypia of the glandular epithelium is also seen compared to the healthy tissue.

Figures 6(c) and 6(d) show the emission spectra obtained for normal and IBD specimens for both excitation wavelengths. For 375 nm excitation, the emission spectrum is shifted to the red for IBD specimens compared to normal, but the shift in mean emission wavelength

#194923 - $15.00 USD Received 31 Jul 2013; revised 11 Oct 2013; accepted 26 Nov 2013; published 16 Jan 2014

was not found to be statistically significant ($p = 0.06$). The spectrally resolved mean fluorescence lifetimes are shown in Figs. 6(e) and 6(f). With 375 nm excitation the mean fluorescence lifetime observed in IBD was longer than that of normal tissue in all spectral channels and this difference appeared to be greater for longer emission wavelengths. Thus, for this excitation wavelength we calculated the spectrally averaged mean fluorescence lifetime over a reduced spectral emission range of 494-556 nm as this gave the greatest contrast (see Fig. 6(g)).

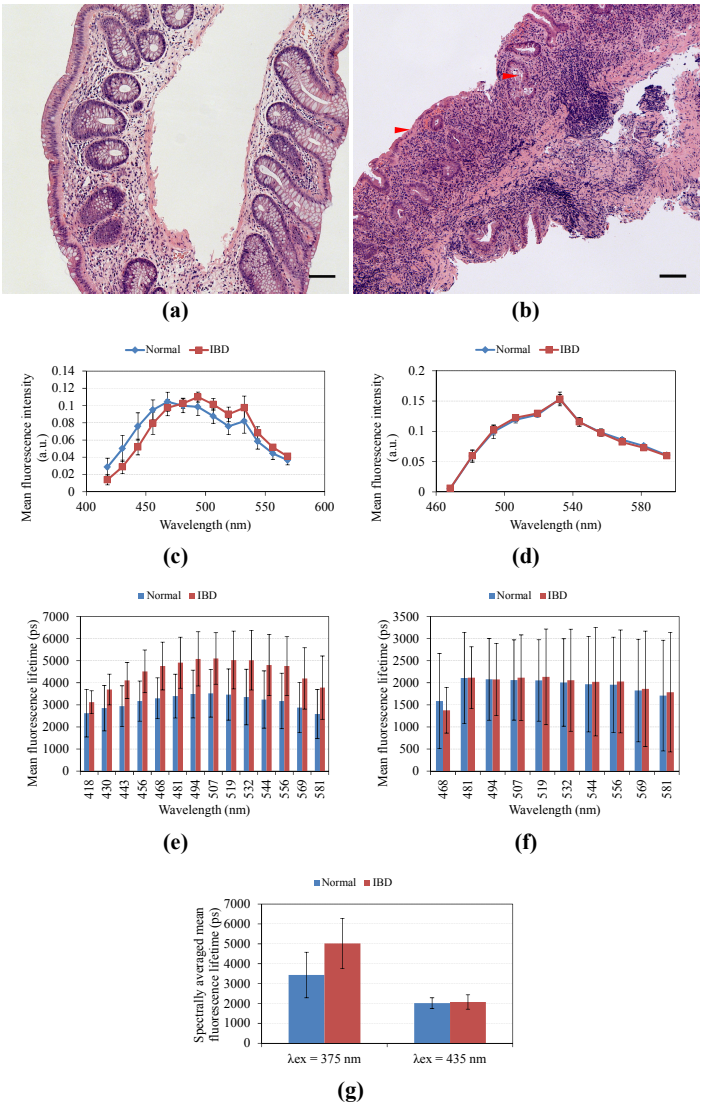

Fig. 6. Comparison of normal tissue and IBD specimens. (a) & (b) show an exemplar H&E stained histological sections of biopsy samples obtained from one patient of (a) normal colonic mucosa and (b) IBD tissue (ulcerative colitis) respectively. Scale bar represents 100 μm, see text for description of arrowheads. (c) & (d) show the mean normalized fluorescence emission spectra obtained with 375 nm and 435 nm excitation, respectively. (e) & (f) show the spectrally resolved mean fluorescence lifetimes with 375 nm and 435 nm excitation, respectively. (g) shows the spectrally averaged mean fluorescence lifetime for both groups and for both excitation wavelengths. The spectrally averaged mean fluorescence lifetime for 375 nm excitation was obtained using the emission spectral range 494-556 nm. The error bars represent ± 1 standard deviation in all panels.

#194923 - $15.00 USD Received 31 Jul 2013; revised 11 Oct 2013; accepted 26 Nov 2013; published 16 Jan 2014

Figure 7 shows the shift observed in the spectrally averaged mean fluorescence lifetime for each IBD sample investigated measured with respect to normal tissue obtained from the same patient (paired analysis). With 375 nm excitation, the fluorescence lifetimes of all four IBD samples are longer than those of the nearby normal colon tissue (mean $\Delta\tau$ = 983 ± 289 ps) but this shift was not found to be statistically significant using the Wilcoxon signed rank test (p = 0.125). We also investigated the paired shift in mean fluorescence emission wavelength between IBD and healthy tissue (mean $\Delta\lambda$ = 6.9 ± 6.6 nm, p = 0.25), which was also not statistically significant. The lack of statistical significance is due to the relatively large standard deviations on the spectral and lifetime shifts and the small number of measurements made for this disease type. Further measurements would be needed to establish if the trends observed are significant. It is also worth noting that the shifts in the mean fluorescence emission wavelength and the spectrally averaged mean fluorescence lifetime were correlated (R^2 = 0.90). Additionally, the relative error for the mean shift in spectrally averaged mean lifetime was a factor of 3.4 times smaller than the relative error for the mean shift in mean emission wavelength.

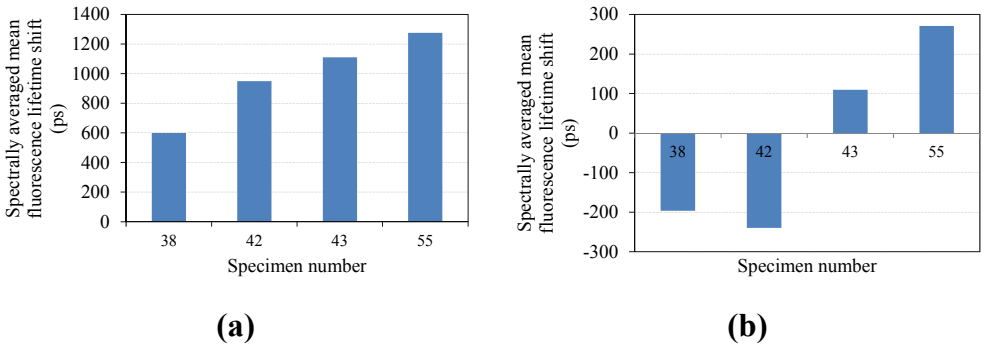

Fig. 7. Bar graphs showing the shift in the spectrally averaged mean fluorescence lifetime observed in all IBD samples relative to a sample of healthy tissue from the same patient. (a) & (b) show lifetime shifts obtained with 375 nm and 435 nm excitation respectively. The lifetime shift for 375 nm excitation was obtained using the spectrally averaged mean lifetime calculated over the emission spectral range 494-556 nm.

#194923 - $15.00 USD Received 31 Jul 2013; revised 11 Oct 2013; accepted 26 Nov 2013; published 16 Jan 2014

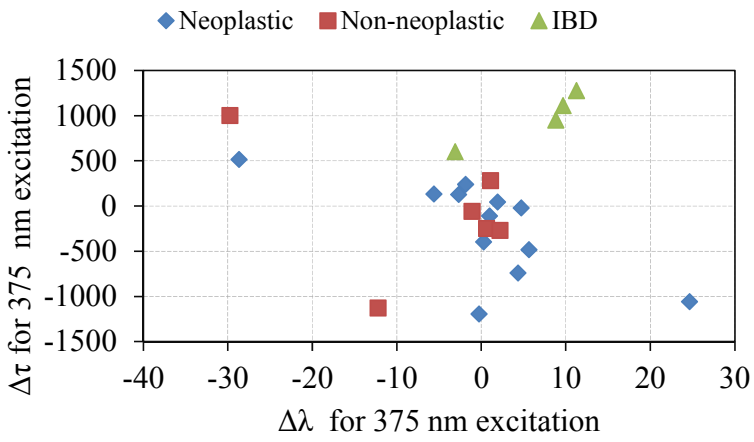

(a)

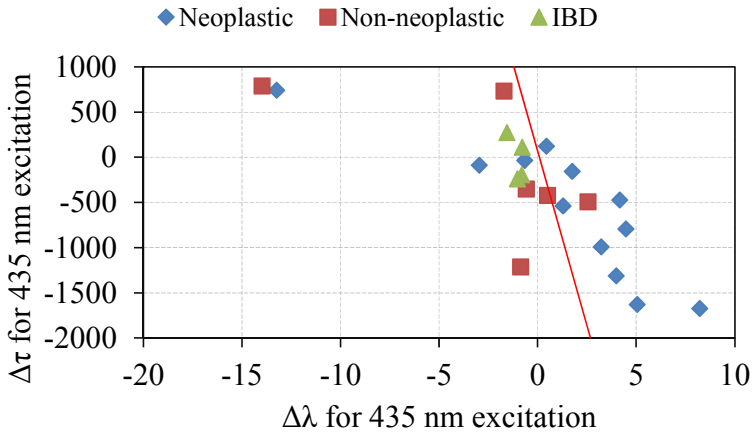

(b)

Fig. 8. Summary of all measured shifts in mean fluorescence emission wavelength and spectrally averaged mean fluorescence lifetime for (a) 375 nm and (b) 435 nm excitation wavelengths. The lifetime shift for 375 nm excitation was obtained using the spectrally averaged mean lifetime calculated over the emission spectral range 494-556 nm for all points.

Figure 8 shows summary plots of all paired measurements of shift in mean fluorescence lifetime against shift in mean emission wavelength for both excitation wavelengths. Paired measurements between two regions of normal tissue would be expected to cluster around the origin. However, it was not possible to obtain such specimens in this study and it was therefore not possible to compare the distribution of normal-normal tissue measurements with those obtained from normal-diseased tissue. Polyp specimens tend to show a decrease in the 435 nm excited spectrally averaged fluorescence lifetime and IBD specimens show an increase in the 375 nm excited spectrally averaged fluorescence lifetime as already discussed in the figures above. The red line in Fig. 8(b) indicates a potential decision line between neoplastic and non-neoplastic polyps, which in this case provides a sensitivity/specificity of

#194923 - $15.00 USD Received 31 Jul 2013; revised 11 Oct 2013; accepted 26 Nov 2013; published 16 Jan 2014

75%/83%. This discrimination mainly makes use of the shift in fluorescence emission wavelength rather than the shift in fluorescence lifetime.

5. Discussion

For "normal" colon (Figs. 2(a) and 2(b) and Fig. 6(a)), our study found no statistically significant variation for either of the excitation wavelengths employed in the mean fluorescence emission wavelength or spectrally averaged mean fluorescence lifetime between tissue from patients presenting polyps or IBD or between tissues from different regions of the colon. We would have expected to see contrast based on the known variations in the structure and composition of these tissues, as segmental variations in normal colon morphology from proximal to distal segments – following the sequence caecum, right colon, transverse colon, left colon, rectum – are well known [52]. From the caecum to the rectum there is a gradual significant decrease in the diameter of the crypts, the number of crypts per unit area and the inner intestinal circumference. There is also an increase in thickness of the mucosa from the caecum (0.5 mm) to the rectum (1 mm). Furthermore, crypts are deeper in the rectum and sigmoid colon than they are in the proximal part of the colon. In addition, it must also be considered that patients with IBD have been variably subjected to medical therapy with steroids, immunomodulators, antibiotics and biologics, which might be responsible for further changes in the mucosal layer thickness/permeability across the entire colon compared to that of untreated patients (i.e. those with polyps). We did observe small changes in emission spectral profile and fluorescence lifetime for these different tissue types but these differences were not statistically significant. This is likely to be due to the relatively small number of specimens in each group. A study on a larger number of specimens would be needed to see if this is true.

Neoplastic polyps are characterized by the presence of epithelial dysplasia and are precursors to colorectal cancer. The histological hallmarks of dysplasia include: the presence of hyperchromatic, elongated and stratified nuclei; highly disorganized architecture; abundant and unregulated epithelial proliferation; mucosal thickening; crypt enlargement; "back to back" aspect of dysplastic cells; lamina propria displacement; a reduction in the number of goblet cells; and aberrant crowded tubular or tubulovillous crypts lined by elongated cigar-shaped cells with narrowing of the crypt lumen (Fig. 4(a)). These changes are normally most pronounced at the head of the polyp (intraluminal protruded portion). The increase in cell density and collagen content in these tissues may cause an increase in optical scattering and the increase in thickness may reduce the contribution of fluorescence signal from lower tissue layers (lamina propria and basal membrane) [53, 54]. Multiphoton microscopy has been used to show that dysplastic epithelium typically displays a higher redox ratio due to increased cellular metabolism [55]. The other expected change between normal colon and polyps is the hemoglobin concentration, which is on average 6 times higher than in normal mucosa [14].

Non-neoplastic polyps can be divided into hyperplastic and inflammatory. Hyperplastic polyps consist - when seen in cross-section - of piled up goblet cells creating an uneven surface architecture (Fig. 4(b)). The most distinctive histological features of inflammatory polyps are hyperplasia of the epithelium and of the lamina propria, mixed inflammatory infiltrates, and erosion.

For 375 nm excitation we expect the dominant tissue fluorophores within the mucosa to be collagen types I-IV and intracellular nicotinamide adenine dinucleotide phosphate (NAD(P)H). Collagen type IV is primarily found in the linings surrounding the colonic crypts (basal membranes), whereas collagen types I-III are predominant in the stroma of the lamina propria [56, 57]. Collagen fluorescence is particularly complex and a range of values are reported in the literature, e.g [58, 59], and recent measurements of type II collagen obtained with an instrument similar to that used here showed a peak emission wavelength of 390-430 nm and a mean fluorescence lifetime of approximately 10 ns for excitation at 355 nm [60]. NADH has a peak emission wavelength of 460 nm and a mean fluorescence lifetime of

#194923 - $15.00 USD Received 31 Jul 2013; revised 11 Oct 2013; accepted 26 Nov 2013; published 16 Jan 2014

440 ps in its free state [61] and longer decay components typically in the range ~2-2.5 ns when protein bound [62]. Our results show a peak fluorescence emission wavelength of 470 nm that is broadly consistent with the fluorescent signal being a combination of collagen and NAD(P)H fluorescence. The fluorescence lifetime measured in this study in the range 3-3.5 ns is also broadly consistent with a combination of the longer decay components found for collagen and those of free and protein-bound NAD(P)H.

In IBD, the intestine is chronically infiltrated by inflammatory cells and in the presence of active disease the epithelium can be severely damaged and frayed (goblet cell and mucin depletion), leaving large exposed areas of underlying connective tissue (Fig. 6(b)). In addition, lymphocytes can cause degradation of collagen [63], the crypts are damaged by intense infiltration of neutrophils (crypt abscesses) and crypt architecture appears distorted. Crypts are unequally spaced and surrounded by an interstitial matrix fully infiltrated by inflammatory cells (neutrophils, lymphocytes and plasma cells). Erythrocytes extravasated from capillaries of the lamina propria may also be present. Loosening of the interstitial space and small crypt openings are also observed. Endoscopically, the mucosa is grossly denuded, with often active bleeding on the surface.

The increase in exposed connective tissue would be expected to increase the contribution of mucosal collagen fluorescence measured by the fiber-probe for excitation at 375 nm and therefore to produce a corresponding increase in the mean fluorescence lifetime (due to the longer mean fluorescence lifetime of collagen compared to NAD(P)H). We do see an increase in the mean fluorescence lifetime observed for IBD, as shown in Fig. 6(g), although this was not found to be statistically significant. However, an increase in the contribution of collagen fluorescence to the signal might also be expected to decrease the mean fluorescence emission wavelength but here we observed an increase - although this was not statistically significant.

In IBD, the metabolic pathway is still not completely understood due to differences in disease states (acute, chronic, active, quiescent) and the wide variation of both metabolic and structural factors involved, such as cytokines secretion, epithelia destruction and regeneration, inflammatory cells infiltrates, autophagy, etc [64, 65]. It is therefore difficult to predict the changes in intracellular AF. Reduced epithelial redox ratios have previously been measured in inflammatory cervical epithelial tissues [63]. Another factor to consider is that the mean penetration depth of light in IBD tissue may be affected by the typically decreased concentration of hemoglobin, which would occur for both diseased and normal samples taken from the same patient given the systemic nature of anemia.

For 435 nm excitation we expect the dominant fluorescence signal to be due to intracellular flavins within the mucosa with perhaps some additional signal from mucosal collagen, which can be excited at this wavelength [66]. The fluorescence emission spectra peak measured in this study at ~530 nm is broadly consistent with the emission spectra of flavins [67] and collagen [66]. In a paired analysis of normal and lesional specimens obtained from the same region of colon, we found that 435 nm excitation of neoplastic colonic polyps provides a statistically significant difference in the spectrally averaged mean fluorescence lifetime (shorter) compared to healthy tissue. This shift in mean fluorescence lifetime was found to be correlated ($R^2 = 0.71$) with a shift in mean emission wavelength. The changes in fluorescence emission spectrum and lifetime might be explained by changes in the ratio of free:protein-bound flavin fluorescence [68, 69] or by changes in the ratio of intracellular flavin fluorescence to collagen fluorescence. We also applied statistical tests to the difference between lesion and normal tissue for each of decay parameters derived from the double exponential analysis, i.e. τ_1, τ_2 and the initial fraction of fluorescence in the short decay component, $a_1/(a_1 + a_2)$, which were all spectrally averaged in the same way as the mean fluorescence lifetime. Of these parameters, only the paired difference in spectrally averaged τ_2 between neoplastic polyp and normal tissue for 435 nm excitation was found to be statistically significant.

#194923 - $15.00 USD Received 31 Jul 2013; revised 11 Oct 2013; accepted 26 Nov 2013; published 16 Jan 2014

To date there are relatively few reports of AFL studies in the colon. Only one study – by Mycek *et al*. [21] – has investigated single point measurements of AFL on colonic polyps at 337 nm excitation. However, while this was the first study in the human colon that demonstrated differences in fluorescence lifetime decay between non-dysplastic and dysplastic tissue, it was mainly carried out to assess the ability of time-resolved AF spectroscopy in distinguishing between adenomatous and non-adenomatous polyps and no measurements from normal tissue were presented. Nevertheless, adenomas showed faster average decays than those of non-adenomas (9300 ± 400 ps vs. 10500 ± 700 ps), where non-adenomas comprised 6 hyperplastic polyps, 3 mucosal prolapses, 1 lymphoid aggregate, and 1 aberrant crypt focus. In the study presented here, we also observed shorter spectrally averaged decays for neoplastic compared to non-neoplastic polyps for either excitation wavelength although these differences were not statistically significant. We note that the shorter excitation wavelength (337 nm) used by Mycek *et al.* means that their work and our results presented should be compared with caution.

Although we kept the time between tissue removal and autofluorescence measurements to below 10 minutes for all specimens, there are a number of potential changes that may occur to the tissue during this time. The blood volume and/or relative concentration of oxyhemoglobin may decrease and the tissue may experience geometrical changes post excision, e.g. shrinkages, tissue curling or crush artifacts and/or changes in thickness of the colonic mucosa layers caused by the biopsy forceps or diathermy [33, 70] which could affect the absorption of the excitation beam, the tissue volume sampled by our instrument and attenuation of the emitted fluorescence. Changes in tissue oxygenation could also affect the metabolic state of cells. These factors could all potentially impact the measured autofluorescence lifetimes. However, the measurement time for normal/diseased pairs in this study was always reasonably well-matched and it is likely that any change to *ex vivo* tissue fluorescence would affect all areas of a sample uniformly and so would be unlikely to alter the relative lifetime contrast between normal and neoplastic tissue [50].

We note that there are a few published studies of how AF signals can change following resection. AF in colonic tissue from intracellular fluorophores such as NAD(P)H has been reported to decay *ex vivo* over a time scale of 118 minutes due to tissue deoxygenation, while the AF from collagen and flavins remained relatively constant [33]. In addition, similar AF intensity and spectral line shapes to that of *in vivo* tissue have been reported for freshly excised tissue in a hamster cheek pouch model [71]. In a study of ischaemic mouse skin by Palero *et al.* [72] using spectrally resolved multiphoton microscopy, the change in fluorescence intensity was reported to increase by 71% compared to baseline over approximately one hour and the change in peak emission wavelength shifted from 456 nm to 450 nm after 20 minutes. It is clear that caution should be exercised when trying to extrapolate *ex vivo* findings to what could be expected *in vivo*. Nonetheless, *ex vivo* measurements are a useful first step to investigating the contrast that is likely to be seen *in vivo*.

6. Conclusions

Optically-assisted diagnosis could be important for medical conditions where biopsies are still required to confirm and characterize the presence and stage of disease. One such example is colonic surveillance for proliferative or inflammatory diseases, where an optical biopsy could enable real-time diagnosis during endoscopy, thereby avoiding multiple and random unnecessary biopsies. Discrimination between dysplasia and inflammation is still one of the most important dilemmas in GI endoscopy.

We have presented an *ex vivo* study of time-resolved autofluorescence spectra of freshly biopsied/removed colonic tissue samples collected from patients undergoing endoscopy as part of their clinical investigation. This was undertaken with a compact fiber-optic coupled time-resolved spectrofluorometer utilizing all-solid-state picosecond diode lasers. In a paired

#194923 - $15.00 USD Received 31 Jul 2013; revised 11 Oct 2013; accepted 26 Nov 2013; published 16 Jan 2014

analysis between normal tissue and neoplastic colonic polyps obtained from the same patient, the decrease in 435 nm excited spectrally averaged mean fluorescence lifetime measured over all patients was found to be statistically significant (mean $\Delta\tau = -570 \pm 740$ ps, n = 12, p = 0.021). If we exclude one sample where it was not possible to obtain a normal sample from the same region of colon, then the level of statistical significance increases (mean $\Delta\tau = -690 \pm 640$ ps, n = 11, p = 0.0049) and the increase in mean emission wavelength also becomes statistically significant (mean $\Delta\lambda = 2.6 \pm 3.0$ nm, n = 11, p = 0.019). The shift in spectrally averaged mean fluorescence lifetime was found to be correlated with the shift in emission spectrum ($R^2 = 0.71$). While non-neoplastic polyps showed a mean difference in mean fluorescence lifetime of -620 ± 400 ps compared to normal tissue obtained from the same region of colon (n = 4), this was not found to be statistically significant for this small sample size.

With respect to discriminating between inflammation and normal tissue, we note that there seemed to be an increase in autofluorescence lifetime for inflamed tissue (IBD) compared to normal tissue but the positive lifetime differences observed were not statistically significant for the small number (n = 4) of IBD specimens studied The increase in 375 nm excited fluorescence lifetime (mean $\Delta\tau = 983 \pm 289$ ps) was correlated ($R^2 = 0.90$) with an increase in fluorescence emission wavelength ($\Delta\lambda = 6.9 \pm 6.6$ nm).

If the changes in mean autofluorescence lifetime and emission wavelength of 435 nm excited fluorescence are combined, then the discrimination of neoplastic from non-neoplastic polyps with a modest sensitivity/specificity of 75%/83% is achieved. Further work is required to see if this can be improved through the use of e.g. other excitation wavelengths, or combinations of fluorescence spectroscopy with other non-invasive optical techniques.

Acknowledgments

This research was funded by the UK Engineering and Physical Sciences Research Council (EPSRC, grant references: EP/F040202/1 and EP/IO2770X/1). The authors gratefully thank the Department of Histopathology of Imperial College Healthcare NHS Trust for their assistance in managing and storing tissue for this study, Mr Keith Wilson and the Department of Clinical Engineering at Charing Cross Hospital for their expert technical assistance, and the staff in the Endoscopy Unit at Charing Cross Hospital for their invaluable assistance with the study. Microscopy of H&E stained sections was performed in the Facility for Imaging by Light Microscopy (FILM) at Imperial College London.